J. Fluid Mech. (1991), vol. 222, pp. 215–230
Printed in Great Britain

Incompressible water-entry problems at small deadrise angles

By S. D. HOWISON[1], J. R. OCKENDON[1] AND S. K. WILSON[2]
[1] Mathematical Institute, 24–29 St Giles, Oxford OX1 3LB, UK
[2] School of Mathematics and Physics, University of East Anglia, Norwich NR4 7TJ, UK

(Received 26 June 1989 and in revised form 11 May 1990)

This paper summarizes and extends some mathematical results for a model for a class of water-entry problems characterized by the geometrical property that the impacting body is nearly parallel to the undisturbed water surface and that the impact is so rapid that gravity can be neglected. Explicit solutions for the pressure distributions are given in the case of two-dimensional flow and a variational formulation is described which provides a simple numerical algorithm for three-dimensional flows. We also pose some open questions concerning the well-posedness and physical relevance of the model for exit problems or when there is an air gap between the impacting body and the water.

1. Introduction

The aim of this note is to review and extend the mathematical techniques available for analysing high-velocity entry flows into a half-space of inviscid fluid (water) in the absence of surface tension in cases where there is a small 'deadrise angle' between the impacting body, be it liquid or solid, and the undisturbed free surface. In these cases the effect of gravity is small over most of the flow, and the contact region between the impacting body and the water half-space expands rapidly. The principal theoretical goal is to find that part of the contact region over which appreciable hydrodynamic forces are exerted.

An excellent review of the subject has been given by Korobkin & Pukhnachov (1988). Also the pioneering but intuitive work of von Kármán (1929) and Wagner (1932) has recently been put on a firmer theoretical basis using matched asymptotic expansions (Cointe & Armand 1987; Wilson 1989; Cointe 1989). This approach forms the basis for our treatment of this class of problems, the first part of which can be regarded as an extension of the results of Cointe & Armand to non-self-similar motion. In addition to this, we will mention the extension of the theory to include three-dimensional impact, air-cushion effects and some questions of stability.

2. Impact by rigid bodies

Mathematically, the best-studied entry problem is the case of a two-dimensional self-similar geometry in which the impacting body is a wedge, gravity and compressibility are neglected throughout, and the effects of any cushioning fluid, such as air, between the wedge and the water are ignored. Theoretical studies of this case have been made by Wagner (1932), Garabedian (1953) and Mackie (1969) among others. The situation is too idealized to be of much practical value but it is

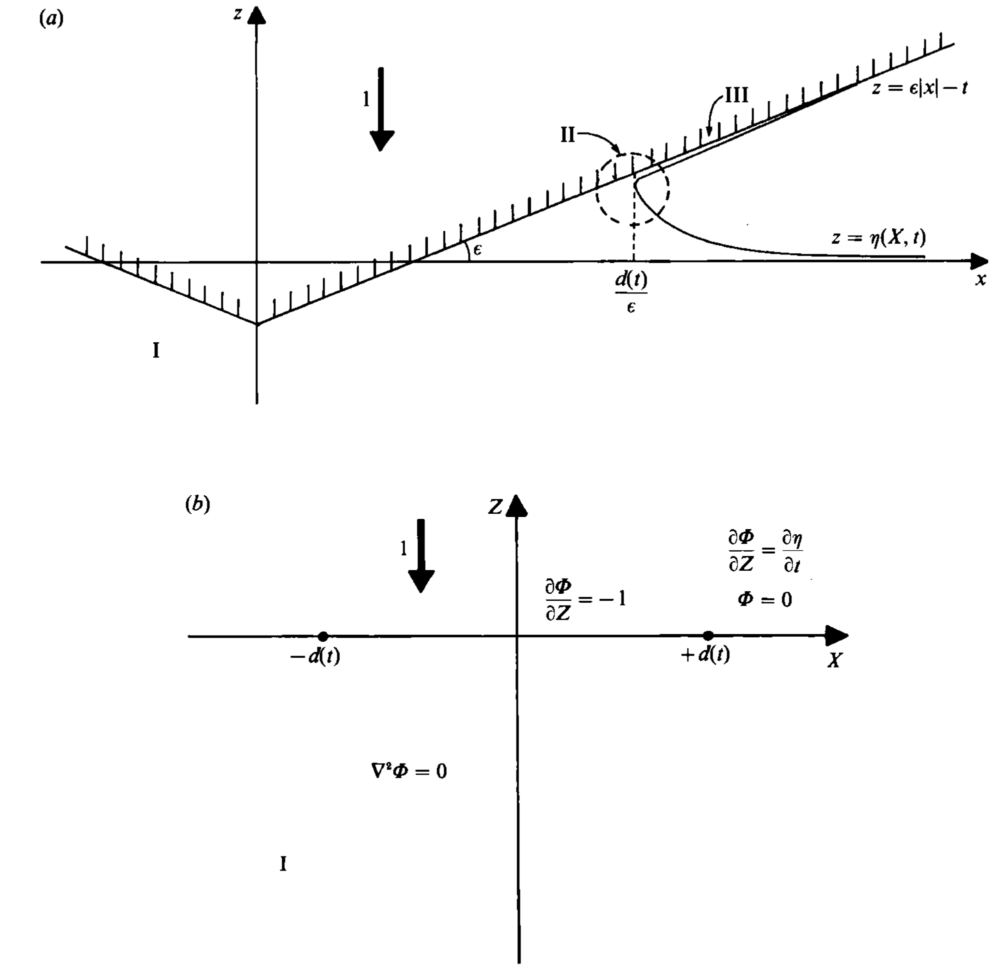

FIGURE 1 (a, b). For caption see facing page.

susceptible to numerical algorithms and experiments (see e.g. Dobrovol'skaya 1969; Hughes 1972; Greenhow 1987) and can give clues about more general cases. Of most interest for our purposes is the small 'deadrise' limit ($\epsilon \ll 1$ in figure 1 a) in which the numerical and experimental evidence of Greenhow (1987) both suggest the formation of thin 'jets' running up the sides of the impacting wedge. Indeed, the principal new phenomenon observed in this configuration is the existence of a very small region of high pressure on the body which enables a precise description of the jet formation mechanism to be given. This high pressure region is implicit in the work of Wagner (1932) and it has also been discussed in a more modern framework of matched asymptotic expansions by Watanabe (1986), Cointe & Armand (1987) and Wilson (1989).

The wedge-entry problem is special in that it has no lengthscale, but, by exploiting the smallness of ϵ, we will be able to construct an approximate solution not just for a wedge with a small deadrise angle but for any impacting body $z/L = f(\epsilon x/L)$ whose slope is small for $|x| \approx O(L)$. By rescaling time, our approach can be modified to describe the initial stages of impact of a general smooth body for times such that the penetration depth is much smaller than the radius of curvature of the body at the

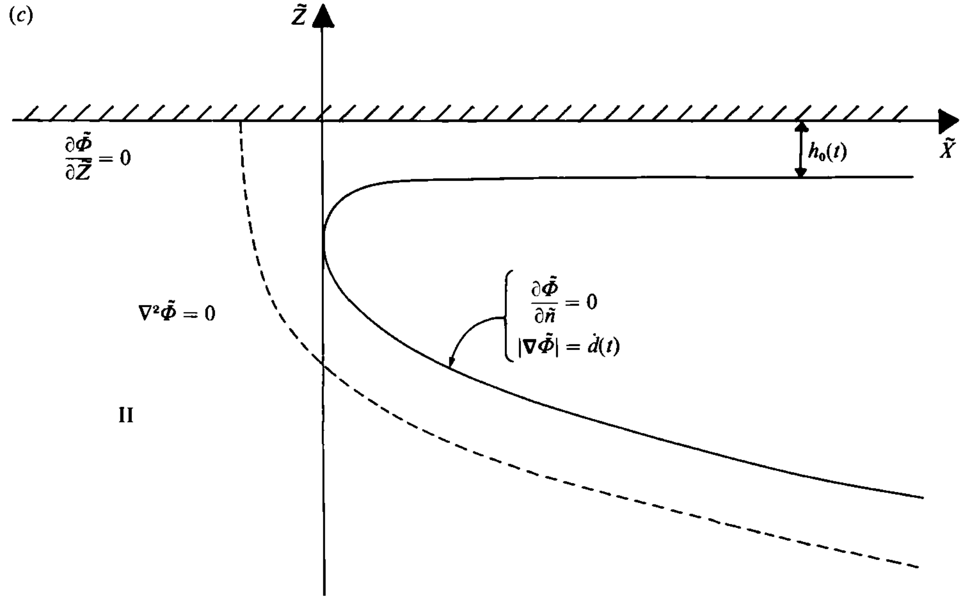

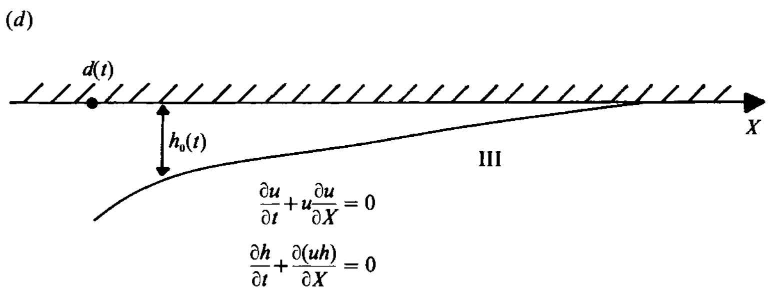

FIGURE 1. (*a*) Fluid entry geometry of a wedge at small deadrise angle. (*b*) Outer flow region. (*c*) Inner flow region. (*d*) Jet region.

point of impact. In such a case it is sufficient to approximate the body by a parabola, or a paraboloid in three dimensions. In these geometries the linearized problem (but not the full problem) has a similarity solution which is discussed by Cointe & Armand (1987) and Armand (1989). In this paper we will solve the linearized problem for a general uniformly shallow body.

We will consider a non-dimensional model in which distances are made dimensionless with the penetration distance L, velocity with a typical impact velocity V_0, time with L/V_0, velocity potential with $V_0 L$ and pressure with the liquid dynamic head corresponding to V_0. Also, we will begin by taking V_0 to be constant and the initial free surface to be flat. The basic idea of the theories presented by Cointe & Armand (1987) and Wilson (1989) is that the flowfield decomposes into the three regions shown in figure 1(*a*).

There is a large outer region I in which, by rescaling $x = X/\epsilon, z = Z/\epsilon$, and the velocity potential $\phi = \Phi/\epsilon$, we find that the liquid responds, to lowest order in ϵ, to the normal impact of a flat plate $|X| < d(t)$ moving in the negative Z-direction with unit speed (figure 1*b*); the corresponding pressure is $O(\epsilon^{-1})$ and the free-surface elevation is of the order of the penetration distance. There is also an inner region II, in which $|X \pm d| = O(\epsilon^2)$, which is a high pressure Kelvin–Helmholtz cavity flow with velocity $O(\epsilon^{-1})$, pressure $O(\epsilon^{-2})$, and extent $O(\epsilon)$ as in figure 1 (*c*). Finally region III is an equally high-velocity jet of length $O(\epsilon^{-1})$, and thickness $O(\epsilon)$, but at a low pressure $O(\epsilon)$ as in figure 1 (*d*).

The size d/ϵ of the equivalent flat plate is determined, as suggested in Wagner (1932), by the condition that the leading-order free-surface elevation as $X \downarrow d$ in the outer flow should equal the wedge elevation as $X \uparrow d$ to within the $O(\epsilon^2)$ lengthscale of region II. In terms of the leading-order outer velocity potential Φ this elevation is

$$\eta(X,t) = \int_0^t \frac{\partial \Phi}{\partial Z}(X,0,\tau)\,\mathrm{d}\tau, \quad |X| > d \tag{1}$$

where

$$\nabla^2 \Phi = 0, \quad Z < 0, \tag{2a}$$

$$\frac{\partial \Phi}{\partial Z}(X,0,t) = -1, \qquad |X| < d(t), \tag{2b}$$

$$\left.\begin{aligned} &\Phi(X,0,t) = 0, \\ &\quad \frac{\partial \eta}{\partial t} = \frac{\partial \Phi}{\partial Z}(X,0,t), \end{aligned}\right\} \quad |X| > d(t), \tag{2c}$$

$$|\nabla \Phi| \to 0 \quad \text{as } X^2 + Z^2 \to \infty, \tag{2d}$$

and $t = 0$ is the time at which the impacting body meets $Z = 0$.† Hence if we write the wedge as $Z = \epsilon f(X)$ at $t = 0$,

$$f(d(t)) - t = \int_0^t \frac{\partial \Phi}{\partial Z}(d(t)+0,0,\tau)\,\mathrm{d}\tau, \tag{3}$$

and, since $\Phi = \mathrm{Re}\{-(Z + (d^2(t) - (X+\mathrm{i}Z)^2)^{\frac{1}{2}})\}$, (3) is simply

$$f(d(t)) - t = \int_0^t \left(-1 + \frac{d(t)}{(d^2(t) - d^2(\tau))^{\frac{1}{2}}}\right)\mathrm{d}\tau.$$

Then, by inversion (Tollmien 1934),

$$d^{-1}(X) = \frac{2}{\pi}\int_0^X \frac{f(\xi)\,\mathrm{d}\xi}{(X^2 - \xi^2)^{\frac{1}{2}}}. \tag{4}$$

We would clearly expect this result to apply to more general symmetric impacting shapes than wedges, and we will say more about this later. Meanwhile we emphasize that the wetted area extends to the tip of the jet and thus exceeds $|X| = d$; it is only for $|X| < d$ in region I and in region II that pressures of $O(\epsilon^{-1})$ or greater are discernible. Indeed, the lowest-order surface pressure in the outer solution is

$$p \sim \begin{cases} \dfrac{1}{\epsilon}\dfrac{d\dot{d}}{(d^2 - X^2)^{\frac{1}{2}}}, & |X| < d, \\ 0, & |X| > d. \end{cases} \tag{5}$$

† It can be shown that (1) and (2) are equivalent to saying that, to lowest order in ϵ, the volume of fluid displaced by the body (i.e. the area of the body below the undisturbed waterline $Z = 0$) is equal to the volume of fluid above the undisturbed waterline as computed from the model for region I; in other words, the flux into the jet is small compared to the net volume displaced.

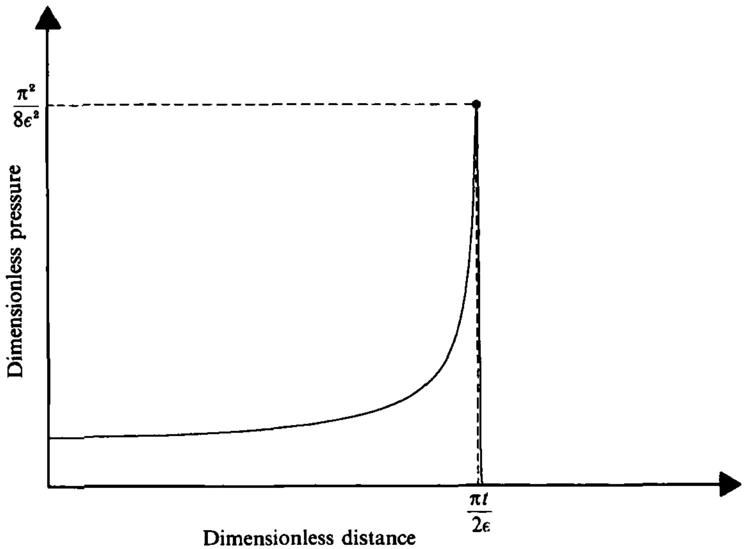

FIGURE 2. Typical pressure distribution on a wedge $y = \epsilon|x|$.

As in Cointe & Armand (1987), we can find the lowest-order solution in region II by writing $X-d = \epsilon^2\tilde{X}$, $Z-\epsilon(f(d)-t) = \epsilon^2\tilde{Z}$, $\Phi-\dot{d}X = \tilde{\Phi}$ to obtain the free-boundary problem shown in figure 1 (*c*). The boundary conditions on the potential function $\tilde{\Phi}$ are such that its normal derivative vanishes and its tangential derivative has modulus $\dot{d}$ on the free boundary, and that $\partial\tilde{\Phi}/\partial\tilde{Z} = 0$ on $\tilde{Z} = 0$. Matching with the first term in region I also gives that, as $\tilde{Z} \to -\infty$,

$$\partial\tilde{\Phi}/\partial\tilde{X} - \mathrm{i}\,\partial\tilde{\Phi}/\partial\tilde{Z} \sim -\dot{d} + (-d/2(\tilde{X}+\mathrm{i}\tilde{Z}))^{\frac{1}{2}}$$

and that the lower branch of the free boundary is described asymptotically by $\tilde{Z} \sim -(2d\tilde{X})^{\frac{1}{2}}/\dot{d}$. We note that this lowest-order problem is invariant under a translation of $\tilde{X}$. Again, as in Cointe & Armand (1987) we can use standard conformal mapping methods (Birkhoff & Zarantonello 1957) to obtain $\tilde{\Phi}+\mathrm{i}\tilde{\Psi} = \dot{d}w(\tilde{X}+\mathrm{i}\tilde{Z})$ where, up to an arbitrary function of t added to w,

$$w = -\frac{h_0(t)}{\pi}\left[\frac{4w'}{(w'+1)^2} + 2\log\left(\frac{w'-1}{w'+1}\right)\right], \tag{6}$$

where $w' = \mathrm{d}w/\mathrm{d}(\tilde{X}+\mathrm{i}\tilde{Z})$ and $h_0(t)$ is the asymptotic jet thickness as we approach region III. Matching with region I gives

$$h_0 = \pi\dot{d}/8d^2 \tag{7}$$

and the pressure distribution on the body in region II is given parametrically to lowest order by

$$p = \frac{\dot{d}^2}{2\epsilon^2}[1-[\xi \pm (\xi^2-1)^{\frac{1}{2}}]^2] \tag{8}$$

where
$$\tilde{X} = \frac{h_0}{\pi}\left[\frac{6+4\xi}{1+\xi} - 4\left(\frac{\xi-1}{\xi+1}\right)^{\frac{1}{2}} + \log\left|\frac{\xi+1}{\xi-1}\right|\right]$$

<table>
<tr><th>$f(X)$</th><th></th><th>$d(t)$</th><th></th></tr>
<tr><td>$|X|$</td><td></td><td>$\frac{\pi t}{2}$</td><td>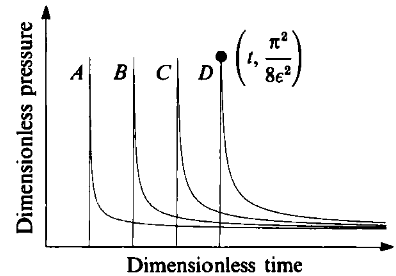</td></tr>
<tr><td>X^2</td><td>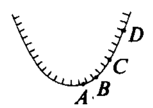</td><td>$(2t)^{\frac{1}{2}}$</td><td>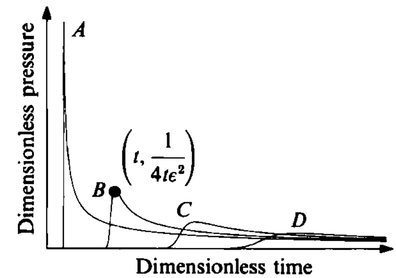</td></tr>
<tr><td>$0, |X| < a$
$|X|-a, |X| \geqslant a$</td><td>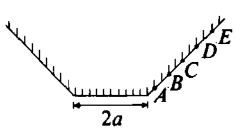</td><td>$(d(t)^2-a^2)^{\frac{1}{2}}-\frac{\pi a}{2}+$
$a\sin^{-1}\left(\frac{a}{d(t)}\right)=\frac{\pi t}{2}$</td><td>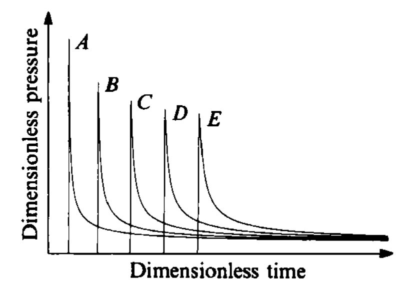</td></tr>
</table>

TABLE 1. Some explicit outer solutions for different f

for $\xi < -1, \xi > +1$ respectively; $|\xi| = \infty$ corresponds to the relative stagnation point $\tilde{X} = 0$ where the maximum pressure occurs.

In (8) we have arbitrarily chosen the relative stagnation point to be at $\tilde{X} = 0$. The problem of calculating the $O(\epsilon)$ correction to the distance of this point from $X = d$ has been raised in Cointe & Armand (1987) and Wilson (1989). As in similar shock location problems in gasdynamics (Lardner 1986), its resolution seems to require a necessarily complicated second-order analysis of the outer solution.

The jet region III is described to lowest order by zero-gravity shallow-water theory and hence the tangential velocity $u(X,t)/\epsilon$ and thickness $\epsilon h(X,t)$ are such that

$$\frac{\partial u}{\partial t}+u\frac{\partial u}{\partial X}=0, \quad \frac{\partial h}{\partial t}+\frac{\partial (uh)}{\partial X}=0. \tag{9a, b}$$

The fact that the mass flow in the jet is only $O(1)$ as $\epsilon \rightarrow 0$ confirms the mass conservation argument leading to (1).

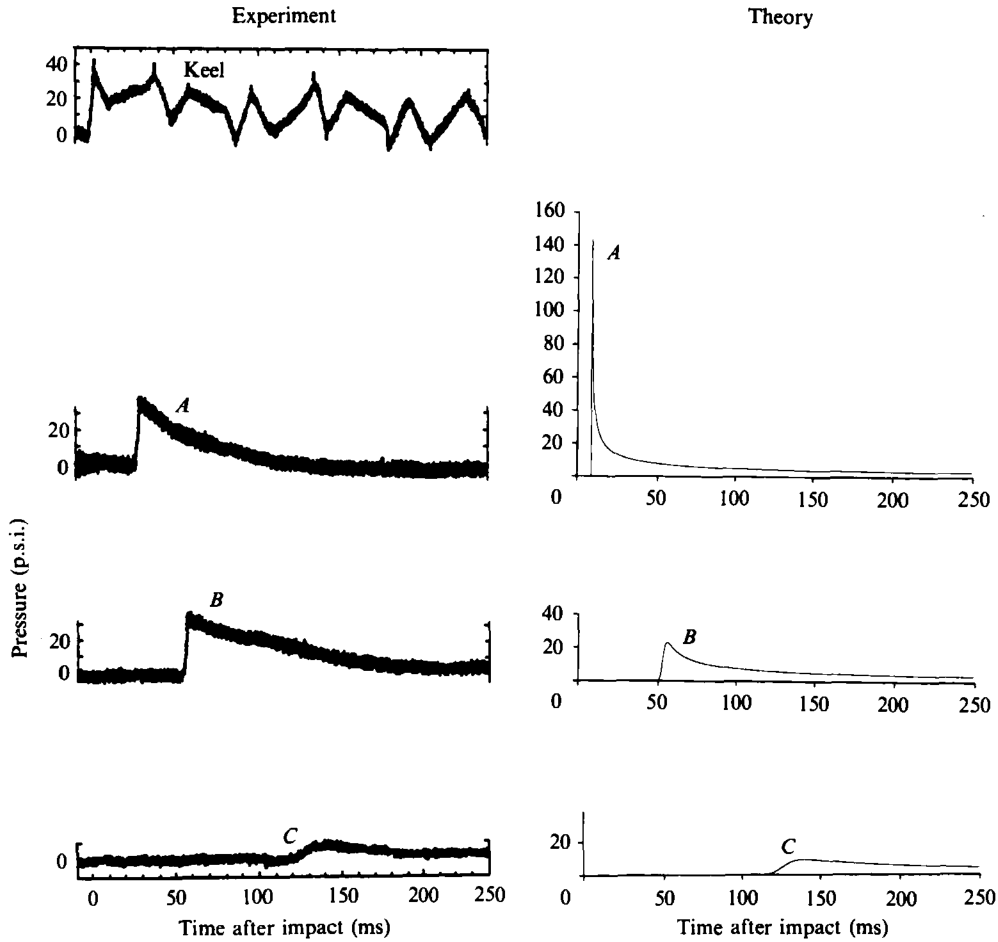

FIGURE 3. Comparison of experimental and theoretical pressure histories. Experimental data from Nethercote *et al.* (1986) with $L = 12$ ft, $V = 20$ ft/s and $\epsilon = 0.707$ so that the dimensionless hull shape is $y = (0.707x)^2$. At the keel the theory predicts an infinite pressure and the oscillations observed experimentally are probably due to air entrapment.

Matching with region II gives $u = 2\dot{d}$, $h = h_0$ at $X = d$, and hence for the wedge

$$u = \pi, \quad h = \frac{1}{4}\left(t - \frac{X}{\pi}\right). \tag{10}$$

To lowest order the jet is only affected by the shape of the impacting body through $d(t)$; however, the pressure on the body in the jet is determined by a higher-order analysis and depends on the body curvature κ through

$$p \sim -\epsilon\kappa h u^2, \tag{11}$$

where κ has the sign of f''. Also, from (4), it is easy to show that shocks (hydraulic jumps) will develop in the solution of (9*a*) if $\ddot{d} < 0$. For curved f, the jet pressure takes its lowest value on the body whenever it is convex and this might provide a criterion for whether or not the jet separates; however, surface tension and gravity

Body shape $Z = \epsilon(f(X, Y) - t)$	Cross-section in plane $Z = 0$	Equivalent flat plate $t = \omega(X, Y)$
Circular cone $f(X, Y) = (X^2 + Y^2)^{\frac{1}{2}}$	Circle $X^2 + Y^2 = t^2$	Concentric circle $\omega(X, Y) = \frac{1}{4}\pi(X^2 + Y^2)^{\frac{1}{2}}$
Elliptic paraboloid $f(X, Y) = \frac{1}{2}(k_1 X^2 + k_2 Y^2)$	Ellipse $k_1 X^2 + k_2 Y^2 = 2t$	Confocal ellipse $\omega(X, Y) = \frac{1}{6}k_1(2 - e^2 - \alpha^2) X^2 \left(X^2 + \frac{Y^2}{1 - e^2}\right)$
Korobkin & Pukhnachov (1988)	$\alpha = \left(1 - \frac{k_2}{k_1}\right)^{\frac{1}{2}}$	$e = \alpha\left(\frac{2 - \alpha^2}{3 - 2\alpha^2}\right)^{\frac{1}{2}}$

TABLE 2. Some known explicit solutions

may have a controlling effect on this phenomenon (see Vanden-Broeck & Keller 1989).

Neglecting the jet pressure, the uniformly valid composite expansion for the pressure exerted on the wedge can now be constructed as in figure 2. The total dimensionless force exerted on the wedge is $O(\epsilon^{-2})$; the leading-order term, which just results from region I is, from (5), $\pi d\dot{d}/\epsilon^2$. Some explicit outer solutions for different f are given in table 1, which also lists schematically the corresponding pressure distributions in $0 < X < d(t)$ as t increases.

As mentioned above these results hold formally for arbitrary rigid body impact of a surface $Z = \epsilon f(X)$ whose deadrise angle is everywhere small and also, with slight modification, to the case when $\eta(X, 0)$ is non-zero but $\eta_X(X, 0)$ is $O(1)$ or when V_0 is non-constant and varies on a timescale L/V_0. Indeed the small-time oblique impact of a circular cylinder on an initially circular free boundary has been analysed in this way by Cointe (1989) as a model for the interaction of spilling breakers with marine structures. However we can in general only treat cases in which $f(X)$ and $\eta(X, 0)$ are even.

Figure 3 compares the leading-order dimensional composite pressure (again neglecting the jet) exerted on a parabolic impacting body with pressure histories measured by Nethercote, Mackay & Menon (1986) for a hull of nearly parabolic cross-section. The agreement is good except on the keel, and this disparity is discussed further in §4. The use of the composite pressure to compute the force on a circular cylinder for small times after impact has been carried out more comprehensively, and compared with experiments, by Cointe & Armand (1987). These authors give a helpful account of the way in which the force in this case falls from its initial, so-called Wagner value (namely $\pi d\dot{d}/\epsilon^2$) towards the value which would be obtained if d were set equal to the semichord in which the x-axis meets the cylinder (the so-called von Kármán value).

We can also write down formally analogous results for the impact of a three-dimensional body $z = f(\epsilon x, \epsilon y)$ except that the inversion (4) is no longer available in general unless there is axial symmetry. Some of the known explicit solutions are listed in table 2, where $y = Y/\epsilon$ and the boundary of the equivalent flat 'disk' in $Z = 0$ is denoted by $t = \omega(X, Y)$. Analytical progress is easiest when there is axial symmetry, in which case the leading-order force on the body is $4\dot{r}r^2/\epsilon^2$, where r/ϵ is the radius of the equivalent disk. For a paraboloid with unit curvature the force is

$6\sqrt{3}t^{\frac{1}{2}}$ which is in fair agreement with the measurements of Moghisi & Squire (1981) for the initial stages of the impact of a sphere, where the force was approximately $8.20t^{\frac{1}{2}}$. Further details of this are given in Wilson (1989).

3. Variational formulation

The three-dimensional version of the model described in §2 can in general only be solved numerically. An easily-implemented algorithm for carrying this out has been suggested by Korobkin (1982), and the transformation he uses has the added bonus of providing a framework in which to discuss the existence, uniqueness and regularity properties of the weak solution of the model, although we will not discuss these aspects here.

In the spirit of the so-called 'Baiocchi transformation' in the theory of variational inequalities (Lions & Stampacchia 1967), we define a displacement potential

$$\Phi^*(X,Y,Z,t) = \int_0^t \Phi(X,Y,Z,\tau)\,\mathrm{d}\tau; \tag{12}$$

a simple calculation shows that

$$\nabla^2\Phi^* = 0, \quad Z<0 \tag{13}$$

with

$$\Phi^*(X,Y,0,t) = 0 \quad \text{for } t<\omega(X,Y). \tag{14a}$$

Also for $t<\omega$,

$$\frac{\partial \Phi^*}{\partial Z}(X,Y,0,t) = \eta(X,Y,t)$$

but, for $t>\omega$,

$$\begin{aligned}\frac{\partial \Phi^*}{\partial Z}(X,Y,0,t) &= \left(\int_0^\omega + \int_\omega^t\right)\frac{\partial \Phi}{\partial Z}\,\mathrm{d}\tau \qquad (14b)\\ &= \eta(X,Y,\omega)-(t-\omega)\\ &= f(X,Y)-t,\end{aligned}$$

from the three-dimensional generalization of (1). Hence as $t\rightarrow\omega\pm 0$,

$$\left.\frac{\partial \Phi^*}{\partial Z}\right|_{Z=0} \rightarrow -t+f(X,Y). \tag{15}$$

Thus the great advantage of working with Φ^* instead of Φ is that $|\nabla\Phi^*|$ is bounded on $t=\omega$ and so Φ^* satisfies the 'complementarity problem' (equivalent to a variational inequality)

$$\nabla^2\Phi^* = 0, \quad Z<0 \tag{16a}$$

$$\Phi^*\left(\frac{\partial \Phi^*}{\partial Z}+t-f\right) = 0 \quad \text{on } Z=0 \tag{16b}$$

with

$$\Phi^* \leqslant 0, \quad \frac{\partial \Phi^*}{\partial Z}+t-f \leqslant 0 \quad \text{on } Z=0. \tag{16c}$$

This provides both a mathematical basis for the expanding plate model (13), (14) and a minimization algorithm for numerical calculations (see for example Elliott &

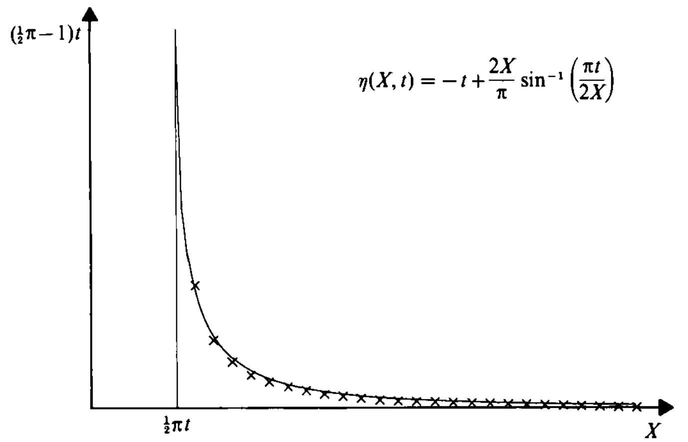

FIGURE 4. Comparison of $\times$, simple finite-element calculation and ——, exact solution of the outer free-surface elevation during a two-dimensional wedge impact at $t = 0.1$.

Ockendon 1982). A rough finite-element discretization for the case of wedge impact is given in figure 4 for comparison with the exact solution which is available analytically from (4) and table 1.

We note that difficulties may arise with this procedure when the curve $t = \omega(X, Y)$ extends to infinity, as may be the case for an approximate model of the impact of a long ship with small deadrise angle at a small angle of attack. However it seems likely that if the angle of attack is much smaller than the deadrise angle the solution may be approximated by a sequence of two-dimensional solutions such as those shown in table 1.

4. Generalized impact problems

4.1. *Air-cushion effects*

The above model neglects several mechanisms which are important in practical problems. Apart from those already mentioned, the most likely explanation for the discrepancy in the pressure readings illustrated in figure 3 for the evolution of a parabolic impact (Nethercote *et al.* 1986) is that air pressure is not negligible in the cushion between the solid and liquid.

The simplest configuration in which to discuss this mechanism is that of a flat-bottomed wedge approaching an initially horizontal free surface as in figure 5. This geometry has been studied experimentally by Driscoll & Lloyd (1982) and theoretically by Verhagen (1967) and Asryan (1972) and we assume the wedge itself has a large enough deadrise angle to allow us to neglect air pressure in $|x| > 1$. If we also neglect air compressibility in $|x| < 1$ then the pressure gradient in the air is proportional to $(\partial V/\partial t) + V(\partial V/\partial x)$ where V is its velocity, which is nearly in the x-direction except near the stagnation point.

Now for a small surface elevation η, the surface water pressure gradient is proportional to the Hilbert transform

$$H\left(\frac{\partial^2 \eta}{\partial t^2}\right) = \frac{1}{\pi}\int_{-\infty}^{\infty} \frac{\partial^2 \eta}{\partial t^2}\frac{d\xi}{(\xi - x)}.$$

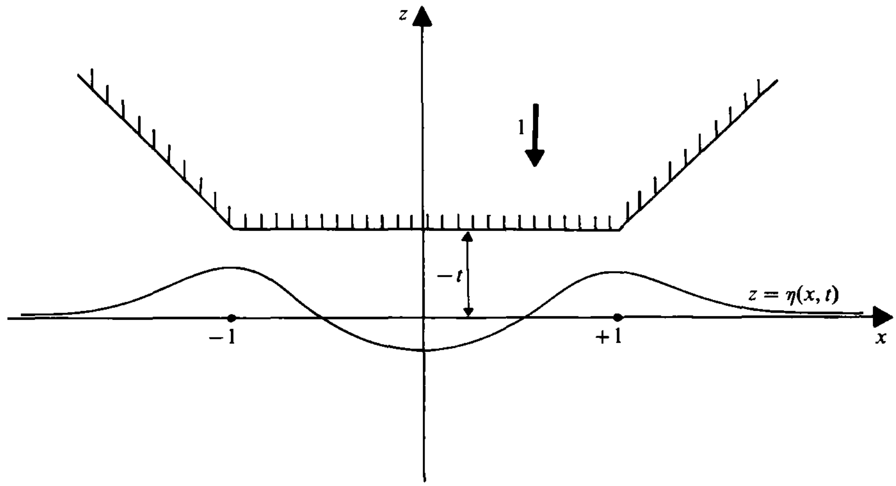

FIGURE 5. Air cushioning geometry.

Hence if we write $\eta = \gamma\theta\tilde{\eta}$ and $V = \gamma\tilde{v}$ where $\gamma \gg 1$ is the initial aspect ratio of the cushion and θ is the air to liquid density ratio, the continuity of pressure on $z = 0$ requires

$$H\left(\frac{\partial^2\tilde{\eta}}{\partial t^2}\right) = \begin{cases} 0, & |x| > 1 \\ \dfrac{\partial\tilde{v}}{\partial t} + \tilde{v}\dfrac{\partial\tilde{v}}{\partial x}, & |x| < 1. \end{cases} \tag{17}$$

The second relation between $\tilde{v}$ and $\tilde{\eta}$ results from mass conservation in the air layer, namely

$$\frac{\partial}{\partial t}(\gamma\theta\tilde{\eta} + t) + \frac{\partial}{\partial x}((\gamma\theta\tilde{\eta} + t)\,\tilde{v}) = 0 \tag{18}$$

for times t such that the air gap thickness is much less than unity. This model is mathematically intractable but as $\gamma\theta \to 0$, we can solve (18) for $\tilde{v}$ and (17) for $\tilde{\eta}$ to obtain

$$\tilde{v} \sim \frac{x}{t}, \quad \tilde{\eta} \sim \frac{2}{\pi}\left[2 + x\log\left(\frac{1-x}{1+x}\right)\right]\log|t| \tag{19}$$

as $t \uparrow 0$.

The fact that $\tilde{\eta} \to \infty$ as $|x| \to 1$ suggests the initiation of the profile sketched in figure 5, but whether this profile is attained in the presence of the nonlinear terms in (18) is unclear. However, the possibility of air escaping through narrow gaps at $|x| = 1$ suggests that air compressibility effects will first become significant there; such effects are discussed in Lewison (1970).

4.2. *Liquid–liquid and liquid–solid impacts*

Several of the ideas mentioned above apply to liquid–liquid and liquid–solid impacts at small deadrise angles. For example, the impact of two identical liquid cylinders along a common generator is identical to the impact of a solid plane on one of the cylinders and can be solved as described before table 1.

For the case of an asymmetric impact with speeds V_1, V_2 as in figure 5, it is easy to

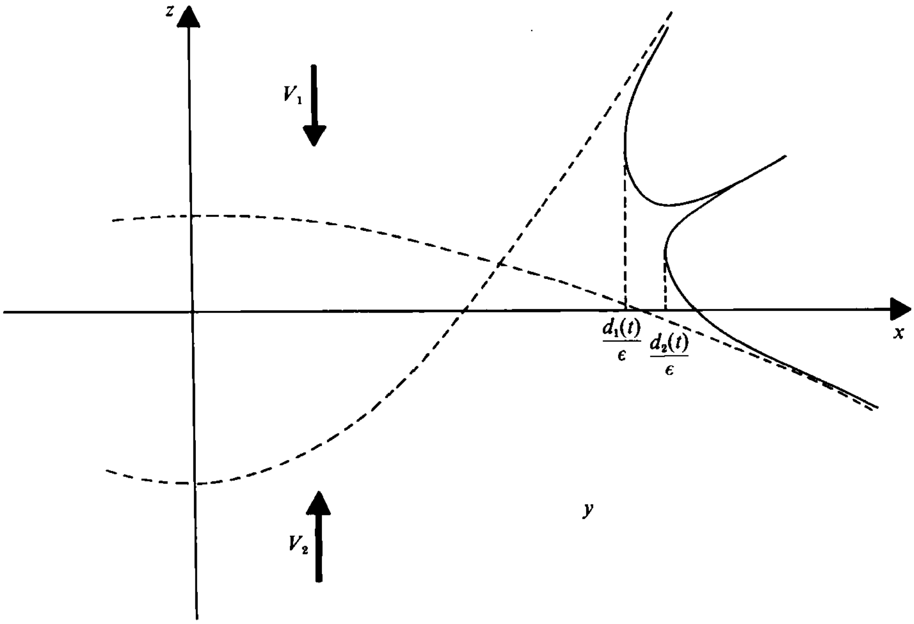

FIGURE 6. Fluid–fluid impact geometry. V_1 and V_2 denote the dimensionless speeds of the impacting fluid masses and the dashed curves are the positions each would have reached in the absence of the other.

see by considering the flow in a frame moving in the Z-direction with speed $\frac{1}{2}(V_2 - V_1)$, in which the contact line is at rest, that the jet angle α is $O(\epsilon)$ only if the high pressure peaks at $X = d_i(t)$ are within $O(\epsilon)$ from each other. However the jet angle α can only be obtained by carrying out the analysis in region II to second order.

5. Stability and exit problems

We will only consider a stability analysis of the model for region I locally in space and time near the 'free boundary' $X = d$. We thus only consider (1)–(3) with a semi-infinite plate $Z = 0, X < d$.

In the two-dimensional solution, Φ has a square-root singularity at the free boundary which means the local velocity is so large that we can neglect the impact speed, but not $\partial\eta/\partial t$, in (2) compared to $\partial\Phi/\partial Z$. When there are variations in the Y-direction, the approximate local model is thus

$$\nabla^2\Phi = 0, \quad Z < 0, \tag{20a}$$

$$\frac{\partial\Phi}{\partial Z} = 0, \quad Z = 0, \quad X < d(t, Y), \tag{20b}$$

$$\phi = 0, \quad \frac{\partial\eta}{\partial t} = \frac{\partial\Phi}{\partial Z}, \quad Z = 0, \quad X > d(t, Y), \tag{20c, d}$$

with $\eta \to 0$ as $X \downarrow d$; also, to match with a two-dimensional solution,

$$\Phi \sim A \operatorname{Re}(-X - \mathrm{i}Z)^{\frac{1}{2}} \tag{21}$$

as $X^2 + Y^2 + Z^2 \to \infty$ where, because we are considering temporal variations which are short on the outer timescale, A is a constant.

This approximate model has an exact travelling wave solution independent of Y in the form

$$\Phi = A\,\mathrm{Re}\,(d-X-\mathrm{i}Z)^{\frac{1}{2}} \tag{22a}$$

$$d = Vt, \quad \eta = -(A/V)(X-d)^{\frac{1}{2}}, \quad X > d, \tag{22b}$$

where V is arbitrary. Like A, V may also be chosen to match with the outer solution and A and V will in fact be related in any particular problem. The precise relationship is unimportant for our analysis but we note that A and V have the same sign and $A > 0$ corresponds to a plate expanding in an impact problem. Also η is negative because the water surface is depressed relative to the X-axis in our local coordinate system.

It is convenient to change to moving axes $\xi = X - Vt$, which changes (20d) into

$$\frac{\partial \eta}{\partial t} - V\frac{\partial \eta}{\partial \xi} = \frac{\partial \Phi}{\partial Z}, \tag{23}$$

and we denote the local boundary $X = d$ by

$$\xi = \delta \cos(ny)\,\mathrm{e}^{\sigma t} + O(\delta^2), \quad n > 0; \tag{24}$$

here δ is a prescribed small number and σ is the growth rate we are seeking. A naive expansion in powers of δ yields

$$\Phi = Ar^{\frac{1}{2}}\sin(\tfrac{1}{2}\theta) + \delta\cos(ny)\cdot\frac{B\,\mathrm{e}^{\sigma t}}{r^{\frac{1}{2}}}\sin(\tfrac{1}{2}\theta)\,\mathrm{e}^{-nr} + O(\delta^2), \tag{25a}$$

$$\eta = -\frac{A}{V}\xi^{\frac{1}{2}} + \delta\cos(ny)\,\eta_1(\xi)\,\mathrm{e}^{\sigma t} + O(\delta^2), \tag{25b}$$

where $r = (\xi^2 + Z^2)^{\frac{1}{2}}$, θ are polar coordinates and B is an undetermined constant. These expansions satisfy (20a–c) and then (23) implies that

$$\sigma\eta_1 - V\frac{\mathrm{d}\eta_1}{\mathrm{d}\xi} = \frac{B\,\mathrm{e}^{-n\xi}}{2\xi^{\frac{3}{2}}}, \tag{26a}$$

so that

$$\eta_1 = \frac{B\,\mathrm{e}^{\sigma\xi/V}}{V}\left[\frac{\mathrm{e}^{-(\sigma/V+n)\,\xi}}{\xi^{\frac{1}{2}}} + \left(\frac{\sigma}{V}+n\right)\int_0^{\xi}\mathrm{e}^{-(\sigma/V+n)\,s}\frac{\mathrm{d}s}{s^{\frac{1}{2}}} + C\right], \tag{26b}$$

after integration by parts. Here C is another constant, and at the moment σ is arbitrary. Now if $\sigma/V > 0$, we can only satisfy the condition that

$$\eta_1 = o(\xi^{\frac{1}{2}}) \quad \text{as } \xi \to \infty$$

if

$$C = -(\sigma/V+n)\int_0^{\infty}\mathrm{e}^{-(\sigma/V+n)\,s}\frac{\mathrm{d}s}{s^{\frac{1}{2}}} = -(\sigma/V+n)^{\frac{1}{2}}\pi^{\frac{1}{2}},$$

whereas if $\sigma/V < 0$, this condition is satisfied even if C remains arbitrary.

However, the expansion (25) is invalid for $r = O(\delta)$, and this necessitates an inner expansion in which $\xi = \delta\xi'$, $Z = \delta Z'$, $\Phi = \delta^{\frac{1}{2}}\Phi'$, $\eta = \delta^{\frac{1}{2}}\eta'$, and (23) becomes

$$\frac{\partial \Phi'}{\partial Z'} = \delta\frac{\partial \eta'}{\partial t} - V\frac{\partial \eta'}{\partial \xi'}. \tag{27}$$

The inner expansion then proceeds

$$\Phi' \sim A\,\mathrm{Re}\,(\cos(ny)\,\mathrm{e}^{\sigma t} - \xi' - \mathrm{i}Z')^{\frac{1}{2}} + \dots \tag{28a}$$

$$\eta' \sim -(A/V)(\xi' - \cos(ny)\,\mathrm{e}^{\sigma t})^{\frac{1}{2}} + \dots, \quad \xi' > \cos(ny)\,\mathrm{e}^{\sigma t}, \tag{28b}$$

the next terms being of $O(\delta)$ apart from any extra terms generated by matching with the outer expansion.† A further matching of the two-term outer with the one-term inner expansion for Φ shows that $B = \frac{1}{2}A$.

Now the inner expansion of (26 *b*) takes the form

$$\eta_1 = \frac{A}{2\delta^{\frac{1}{2}}\xi^{\frac{1}{2}}} + \tfrac{1}{2}AC + O(\delta^{\frac{1}{2}}). \tag{29}$$

The first term in (29) automatically matches the term of $O(\xi'^{-\frac{1}{2}})$ in the expansion of (28 *b*) as $\xi' \to \infty$ but the second term generates a constant of $O(\delta^{\frac{1}{2}})$ with which the next term in (28 *b*) has to match. This would lead to a potential problem for the second term in the expansion for Φ' which would have to satisfy homogeneous Neumann and Dirichlet data on $Z' = 0$, $\xi' < \cos(ny)\,\mathrm{e}^{\sigma}t$, $\xi' > \cos(ny)\,\mathrm{e}^{\sigma t}$ respectively and be such that its normal derivative on $Z' = 0$, $\xi' < \cos(ny)\,\mathrm{e}^{\sigma t}$ had finite integral. The boundary conditions mean that such a function would have to be a combination of square roots of $\xi' + \mathrm{i}Z'$ and no such function has the required finite integral. We conclude that the term $\frac{1}{2}AC$ in (29) is zero; hence if $\sigma/V > 0$, $\sigma/V + n = 0$ which is impossible. Thus σ and V must have opposite signs, which suggests that an expanding plate problem is stable but that an 'exit' problem when $V < 0$ is unstable.

The fact that we are unable to write down a dispersion relation between σ and n is related to the behaviour of the solution of the linear initial-value problem for (20) in which the initial condition $\eta = \Omega(\xi)$, say, at $t = 0$ is imposed instead of (24). We will not pursue the details here but we note that (23) now yields a first-order partial differential equation for the difference between η and $-(A/V)\,\xi^{\frac{1}{2}}$. The characteristics are $\xi + Vt =$ constant, but we need to solve in $\xi \geqslant 0$ and data is prescribed at $t = 0$; hence the problem cannot be solved without some continuation process involving Ω if $V < 0$.

The above analysis suggests there may be marked differences between exit and entry problems. Even though any solution of our expanding plate model can be reversed in time to give the solution of an exit problem with initial conditions identical to those encountered in the evolution of an entry problem, this tells us very little about the evolution of the exit problem for arbitrary initial data. In addition to the stability argument, differences between the two situations are suggested by the facts that

(i) time reversal in an entry problem reverses the sign of the pressure in region I; hence, from table 1, large negative pressures are predicted which could invalidate the model by causing the boundary of the contracting plate to break up;

(ii) the smoothing transformation (12) can still be applied to the exit problem but we can no longer derive the crucial boundary condition (14) in the region traversed by $t = \omega(X, Y)$. This difficulty also prevents us writing down an integral equation corresponding to (3) without some extra physical assumption about the nature of η in this region.

Finally, we note that a formal solution to any exit problem in the absence of gravity is that the body instantaneously loses contact at all points and $\eta(x,t) \equiv \eta(x,0)$. However, further work is needed to see if there is a mathematical interpretation which is in better agreement with the observations of Greenhow (1988).

† The expansion (28) is itself invalid near $\xi' = Z' = 0$ because repeated inner expansions are needed to determine the higher-order terms in the free-boundary position (24).

6. Conclusion

We have presented a brief account of the theory of small deadrise impacts between solids and liquids, assuming for the most part that surface tension, gravity, viscous and compressible effects can be neglected. This enables explicit solutions to be calculated for the pressures exerted on the impacting body in two-dimensional and axisymmetric cases. Moreover, general three-dimensional impacts can be reduced to a variational formulation which is suitable for numerical discretization, and which avoids explicit reference to the boundary of that part of the impacted region where high pressures are exerted.

Although the results of these calculations have been shown to agree quite well with experimental evidence, several of the solutions we have described suggest that some or all of the neglected effects may be important in localized regions. In particular more realistic analyses of the jet tip and of jet separation may be needed. Another important open question concerns the formulation of exit problems which, even in the absence of gravity, do not seem to be well described in the small deadrise limit as time reversals of entry problems.

We are very grateful Mr D. Chalmers and Mr J. Clarke for suggesting this research and to Drs J. Byatt-Smith, M. Greenhow and P. Wilmott for discussions concerning the modelling of splashing and stability respectively. We also acknowledge some very helpful referees' comments, and would like to thank Professor H. Peregrine for pointing out the work of Cointe & Armand. S.K.W. acknowledges financial support from the SERC.

REFERENCES

ASRYAN, N. G. 1972 Solid plate impact on surface of incompressible fluid in the presence of a gas layer between them. *Isv. Akad. Nauk. Arm. SSR Mekh.* **25**, 32–49.

BIRKHOFF, G. & ZARANTONELLO, E. H. 1957 *Jets, Wakes and Cavities*. Academic.

COINTE, R. 1989 Two-dimensional water-solid impact. *ASME J. Offshore Mech. Arc. Engng* **111**, 109–114.

COINTE, R. & ARMAND, J.-L. 1987 Hydrodynamic impact analysis of a cylinder. *ASME J. Offshore Mech. Arc. Engng* **109**, 237–243.

DOBROVOL'SKAYA, Z. N. 1969 On some problems of similarity flow of fluid with a free surface. *J. Fluid Mech.* **36**, 805–829.

DRISCOLL, A. & LLOYD, A. 1982 Slamming experiments – description of facilities and details of impact pressure results. *Rep. AMTE* (H) R82002.

ELLIOTT, C. M. & OCKENDON, J. R. 1982 *Weak and Variational Methods for Free and Moving Boundary Problems*. Pitman Research Notes in Mathematics, no. 59.

GARABEDIAN, P. R. 1953 Oblique water entry of a wedge. *Commun. Pure Appl. Maths* **6**, 157–165.

GREENHOW, M. 1987 Wedge entry into initially calm water. *Appl. Ocean Res.* **9**, 214–223.

GREENHOW, M. 1988 Water entry and exit of a horizontal circular cylinder. *Appl. Ocean Res.* **10**, 191–198.

HUGHES, O. F. 1972 Solution of the wedge entry problem by numerical conformal mapping. *J. Fluid Mech.* **56**, 173–192.

KÁRMÁN, T. VON 1929 The impact of sea plane floats during landing. *NACA TN* 321.

KOROBKIN, A. A. 1982 Formulation of penetration problem as a variational inequality. *Din. Sploshnoi Sredy* **58**, 73–79.

KOROBKIN, A. A. & PUKHNACHOV, V. V. 1988 Initial stage of water impact. *Ann. Rev. Fluid Mech.* **20**, 159–185.

LARDNER, R. W. 1986 Third-order solutions of Burgers' equation. *Q. Appl. Maths* **64**, 293–301.

LEWISON, G. R. G. 1970 On the reduction of slamming pressures. *Trans. RINA* **112**, 285–306.

LIONS, J.-L. & STAMPACCHIA, G. 1967 Variational Inequalities. *Commun. Pure Appl. Maths* **20**, 493–519.

MACKIE, A. G. 1969 The water entry problem. *Q. J. Mech. Appl. Maths* **22**, 1–17.

MOGHISI, M. & SQUIRE, P. T. 1981 An experimental investigation of the initial force of impact on a sphere striking a liquid surface. *J. Fluid Mech.* **108**, 13–146.

NETHERCOTE, W. C. E., MACKAY, M. & MENON, B. 1986 Some warship slamming investigations. *DREA Tech. Mem.* 86/206.

TOLLMIEN, W. 1934 Zum Landestoß von Seeflugzeugen. *Z. Angew. Math. Mech.* **14**, 251.

VANDEN-BROECK, J. M. & KELLER, J. B. 1989 Pouring flows with separation. *Phys. Fluids* A **1**, 156–159.

VERHAGEN, J. H. G. 1967 The impact of a flat plate on a water surface. *J. Ship Res.* **11**, 211–223.

WAGNER, H. 1932 Uber Stoss-und Gleitvorgänge an der Oberflache von Flussigkeiten. *Z. angew. Math. Mech.* **12**, 193–215. (Trans. Phenomena associated with impacts and sliding on liquid surfaces. *NACA Trans.* 1366.)

WATANABE, I. 1986 Analytical expression of hydrodynamic impact pressure by matched asymptotic expansion technique. *Trans. West Japan Soc. Naval Arch.* **71**, 77–85.

WILSON, S. K. 1989 The mathematics of ship slamming. D. Phil. thesis, Oxford University.